Electronic Supplementary Material (ESI) for Journal of Materials Chemistry C.
This journal is © The Royal Society of Chemistry 2017

Supporting Information：

Improved Quality of Electrochemical Polymerized Luminescent Films on Au-Nanoparticles Modified Electrodes: Au-Nanoparticles Induced Interfacial Nucleation and Fast Electron Transfer

Rong Wang[a], Cao Liu[b], Xuehong Zhou[b], Linlin Liu[b*], Yuguang Ma[ab*]

[a] State Key Laboratory of Supramolecular Structure and Materials, Jilin University, Changchun 130012, P. R. China.

[b] Institute of Polymer Optoelectronic Materials & Devices, State Key Laboratory of Luminescent Materials and Devices, South China University of Technology, Guangzhou 510640, P. R. China.

Table of the contents:

1. Experimental Section S2

2. The AFM images of ITO electrode S4

3. The water contact angle of ITO and ITO/Au-2nm electrodes S5

4. The Electrochemical Impedance Spectroscopy of ITO and ITO/Au-2nm electrodes S5

5. The CV curves of ferrocene on ITO and ITO/Au-2nm electrodes S6

6. The Transmittance of ITO and ITO/Au-2nm electrodes S6

7. CV curves of OCBzC on ITO and ITO/Au-2nm electrodes at different scan rates.....S7

8. Electrochemical polymerization and kinetics behavior of OCBzC on different electrodes S7

9. AFM images of ITO/AuNPs electrodes with different thickness AuNPs and their corresponding EP OCBzC films. S8

10. Additional Reference S9

1. Experimental section

Materials

Tetrabutylammonium hexafluorophosphate (TBAPF6, 98%) was purchased from Alfa Aesar which would be recrystallized twice from ethanol and dried for 24 h under vacuum before used. All solvents were purchased from Sigma-aldrich and used without further purification. The synthesis of OCBzC has been previously reported by our group.[1]

Instrumentation

The electrochemical polymerization was performed using a standard one-compartment, three-electrode electrochemical cell attached to a CHI 760D Electrochemical Workstation. Tapping mode atomic force microscopy (AFM) images were taken in air using a Nanoscope III, Digital Instrument system equipped with a 3 μm ×3 μm scanner and a silicon nitride cantilever.X-ray photoelectron spectroscopy (XPS) was carried out ona Kratos Axis Ultra DLD instrument (England) with photoelectrons generated by the non-monochromatic Al Ka irradiation (1486.6 eV). Both low (FAT, pass energy = 160 eV) and highresolution (FAT, pass energy = 40 eV) spectra were recorded. The current density–luminance–voltage (J–L–V) and luminance efficiency–current density (L-J) characteristics were measured in the nitrogen dry box using a Keithley 236 source measurement unit and a calibrated silicon photodiode in the N2 atmosphere dry box. Then the brightness was calibrated using a PR-705 SpctraScan spectrophotometer (Photo Research), which was aligned to the normal direction of emitting surface.

Electrochemical experiments

Cyclic voltammetry (CV) experiments were performed using a standard one-compartment, three-electrode electrochemical cell. A 0.01M Ag/Ag^+ nonaqueous electrode was used as reference electrode. ITO and ITO/AuNPs were used as the working electrode and titanium metal was used as the counter electrode. AuNPs were deposited on ITO by thermo- evaporation in a vacuum chamber with base pressure of 2×10^{-6} mbar and evaporation rate of 0.05 Å s^{-1} to make ITO/AuNPs electrodes. The thickness of AuNPs was measured precisely by the Filtech during evaporation and the size of AuNPs was carefully controlled by the thickness of AuNPs film (the mean diameter of AuNPs-1 nm, 2 nm and 4 nm thickness were about 5 nm, 8 nm and 12 nm, respectively, calculated from AFM images). A mixture of or OCBzC (0.5 mg mL^{-1}) and $TBAPF_6$ (0.1M) with CH_3CN/CH_2Cl_2(V/V=2/3) was used as electrolyte solution. All EP films were prepared by CV mode in the following conditions: using ascan range of -0.50 V～0.86 V, a scan rate of 50 mV s^{-1} andscan cycles of 10 cycles. After the electrochemical deposition process, the resulting film was washed with solvents, to remove any unreactive precursors and supporting electrolytes, and then dried in a vacuum oven.The electrochemical impedance spectroscopy was measured at 0.86V and 10^6～1Hz.

Diffusion coefficient and electron-transfer rate constant measurements

The diffusion coefficients (D_o) and the electron-transfer rateconstants (κ_f) of OCBzC precursor on different electrodes were determined by performing CV and CC experiments attached to a CHI 760D Electrochemical Workstation, respectively. The

Do was calculatedaccording to the Randles–Sevcik equation, where ip is theoxidation peak current of carbazole unit, C_o is the bulkconcentration of the electroactive units and A is thesurface area of the working electrode, which was determined by the AFM.

In the CC experiment, the potential was stepped from0 V to 0.86 V and kept for 6 s to record the Q～t curve, thenthe κ_f was calculated from the Anson equation. All measurements were carried out at room temperature (25℃).

OLEDs fabrication

The device structure was ITO/Au-2nm or w/o/ EP OCBzC film/TPBi (35 nm)/CsF(1nm)/Al (100 nm). The EP OCBzC films was electrochemical deposited on ITO or ITO/Au-2nm substrate, then a 35 nm TPBi films and 1 nmcesium fluoride (CsF) film acted as an electron injection layer and a 100 nm Al cathode layer were thermally evaporated with a base pressure of 3× 10^{-4} Pa. All device fabrication processes are carried out in a N_2-filled glove box

2. The AFM images of ITO electrode

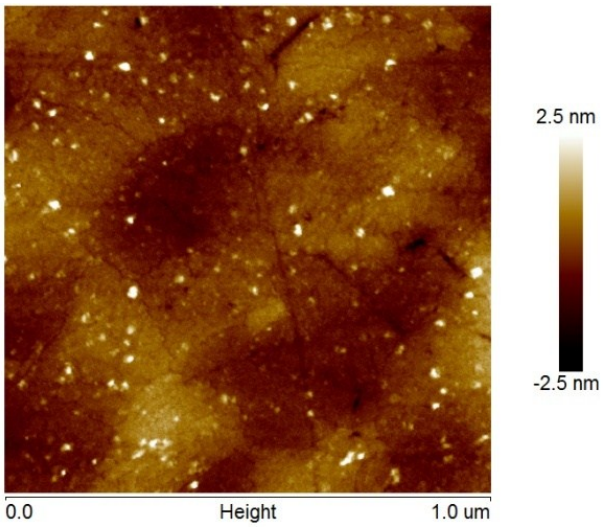

Figure S1. AFM image of ITO electrode.

3. The water contact angle of ITO and ITO/Au-2nm electrodes

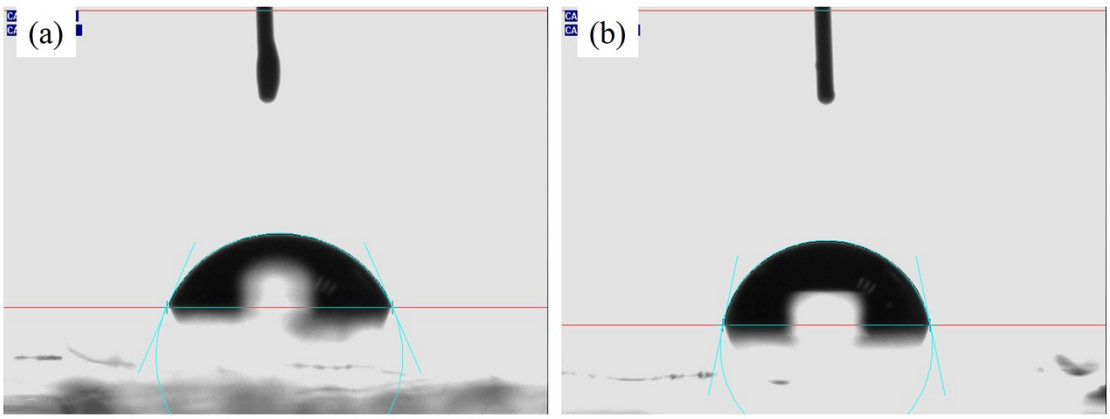

Figure S2. (a) The water contact angle of ITO electrode (66.4°) and (b) the water contact angle of ITO/Au-2nm electrode (78.2°).

4. The Electrochemical Impedance Spectroscopy and Transmittance of ITO and ITO/Au-2nm electrodes

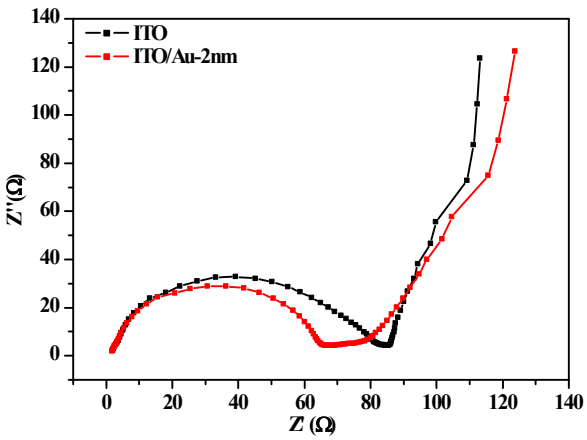

Figure S3. The electrochemical impedance spectroscopy of ITO and ITO/Au-2nm electrodes at 0.86 V and 10^6~1Hz.

5. The CV curves of ferrocene on ITO and ITO/Au-2nm electrodes

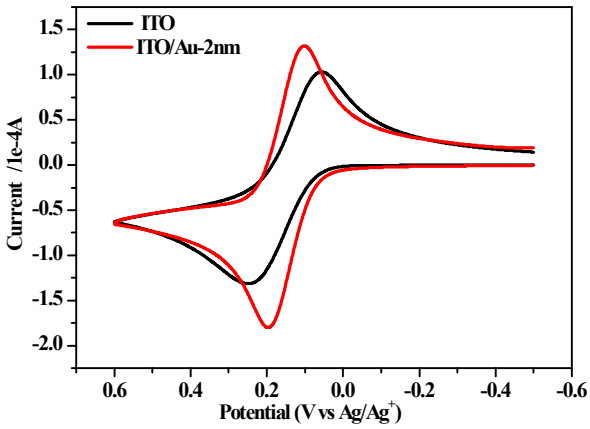

Figure S4. The CV curves of ferrocene on both electrodes. The oxidation and reduce peak potential (Epa, Epc) on ITO electrode were 0.249 V and 0.056 V with a ΔE (ΔE=Epa-Epc) of 0.193 V and a Ipc/Ipa ratio of 91.7%, while on ITO/Au-2nm electrode,the Epa, Epc shift to 0.197 V and 0.101 V and showed a narrowerΔE of 0.096 V and a higher Ipc/Ipa ratio of 97.5%.

6. The Transmittance of ITO and ITO/Au-2nm electrodes

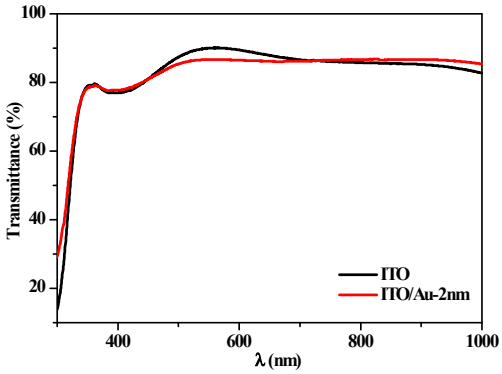

Figure S5. The Transmittance of ITO and ITO/Au-2nm electrodes.

7. CV curves of OCBzC on ITO and ITO/Au-2nm electrodes at different scan rates

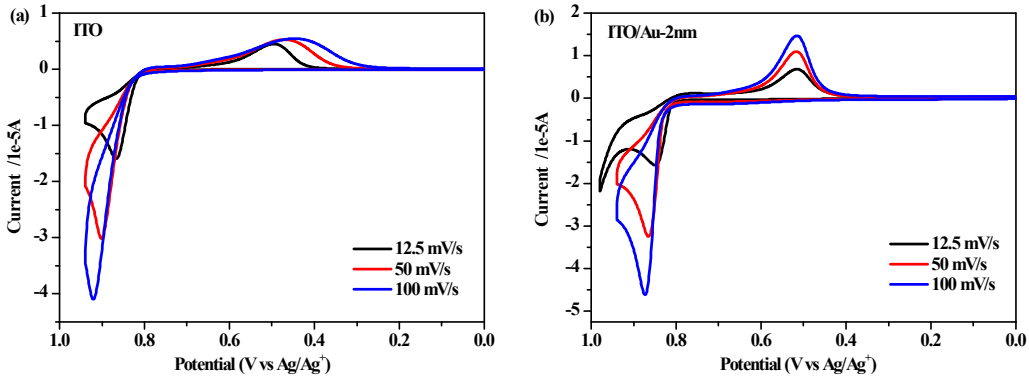

Figure S6. (a) CV curves of OCBzC on ITO electrode at scan rates from12.5 to 100 mV s^{-1} and (b) CV curves of OCBzC on ITO/Au-2nm electrode at scan rates from 12.5 to 100 mV s^{-1}.

8. Electrochemical polymerization and kinetics behavior of OCBzC on different electrodes

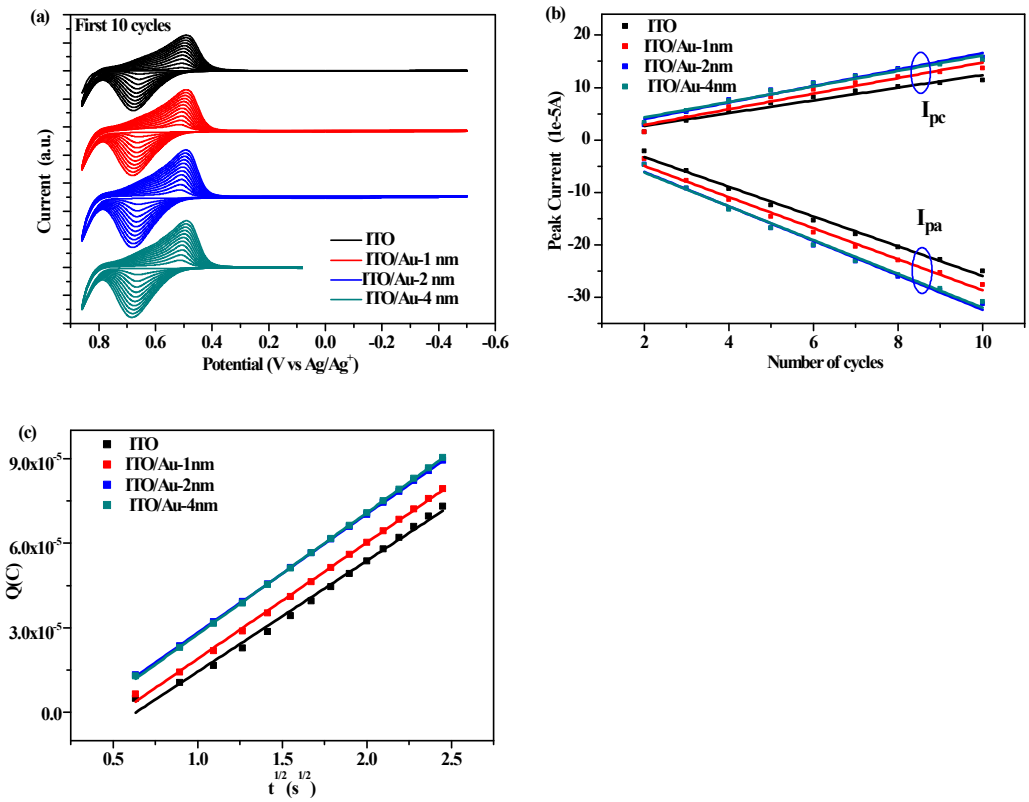

Figure S7. (a) The EP behavior of OCBzC during the first 10 cycles over -0.5～0.86 V

on different electrodes; (b) The variations of theIpa and Ipc of dimeric carbazole with cycle number on different electrodes; (c) The Anson plots (Q vs. $t^{1/2}$) of OCBzC on different electrodes.

9. AFM images of ITO/AuNPs electrodes with different thickness AuNPs and their corresponding EP OCBzC films

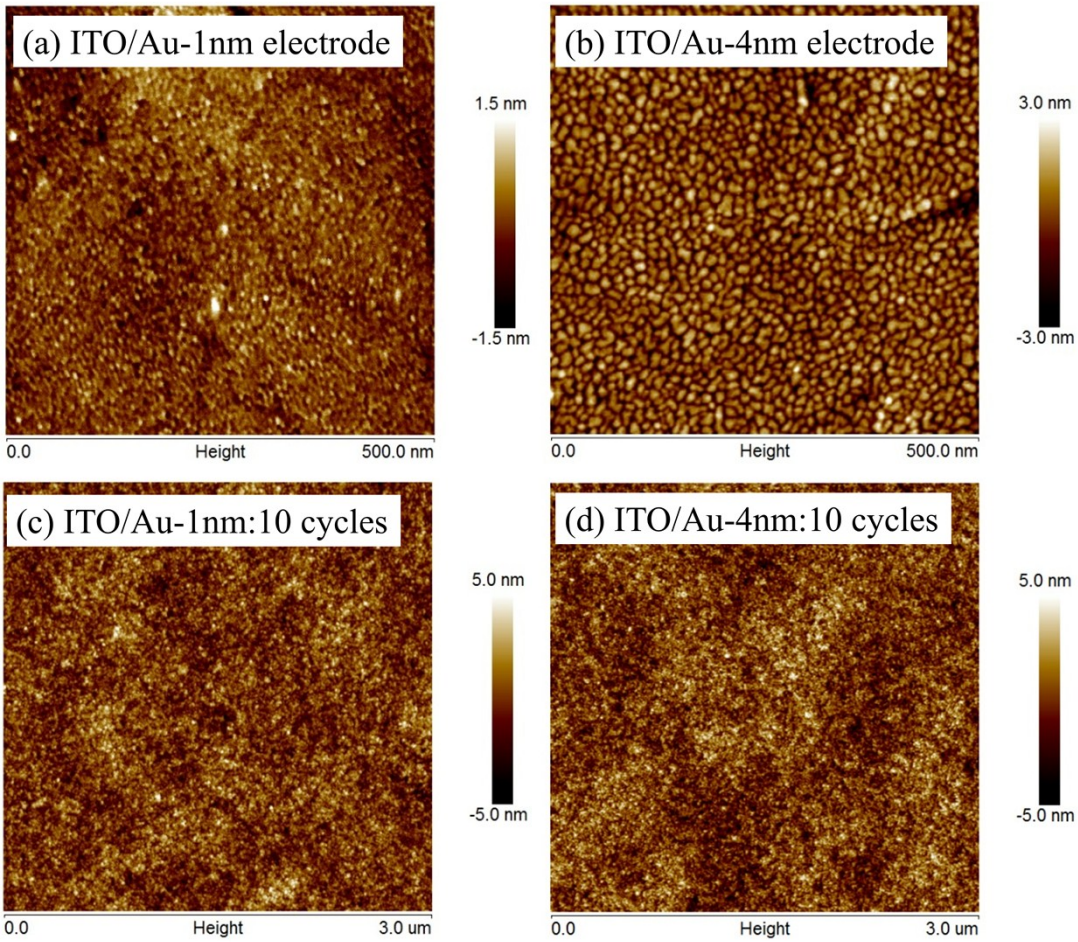

Figure S8. AFM images of ITO/AuNPs electrodes with different thickness AuNPs (a) ITO/Au-1nm; (b) ITO/Au-4nm; AFM images of EP OCBzC films deposited on ITO/ AuNPs electrodes with different diameter AuNPs (c) ITO/Au-1nm; (d) ITO/Au-4nm.

10. Additional Reference

1 L. Yao, S. Xue, Q. Wang, W. Dong, W. Yang, H. Wu, M. Zhang, B. Yang, and Y. Ma, *Chem. Eur. J.*, 2012, **18**, 2707-2714.